buildings

MDPI

Article

Improving the Mechanical Properties of Concrete Mixtures by Shape Memory Alloy Fibers and Silica Fume

Yuanyong Xie [1,*], Harry Far [2,*], Mina Mortazavi [2] and Ahmed M. El-Sherbeeny [3]

[1] Municipal Design Research Institute of Chongqing Design Group Co., Ltd., Chongqing 400020, China
[2] School of Civil and Environmental Engineering, Faculty of Engineering and Information Technology, University of Technology Sydney (UTS), Sydney, NSW 2007, Australia; mina.mortazavi@uts.edu.au
[3] Industrial Engineering Department, College of Engineering, King Saud University, P.O. Box 800, Riyadh 11421, Saudi Arabia; aelsherbeeny@ksu.edu.sa
* Correspondence: htt_011984@cqjzc.edu.cn (Y.X.); harry.far@uts.edu.au (H.F.)

Abstract: Concrete, as one of the most widely applied materials in buildings, has high environmental impacts. Researchers are continually seeking solutions to mitigate these environmental issues while enhancing the mechanical strength and durability of concrete. However, there is a lack of studies on the effect of combining silica fume (SF) as pozzolanic materials and shape memory alloy (SMA) fibers on the mechanical properties of concrete. Moreover, there is very limited research on the influence of these materials on concrete mixtures after primary failure cracks using the secondary compressive strength test. In this research, 0.1, 0.2, and 0.3% SMA and 5, 7.5, and 10% SF were applied and then subjected to compressive strength, splitting tensile strength, flexural strength, secondary compressive strength, and ultrasonic pulse velocity tests. According to the results, 10% SF is more economical, which increases the compressive, splitting tensile, and flexural strength by 14%, 7%, and 10%, respectively. Also, using 0.3% SMA improves the compressive, splitting tensile, and flexural strength by 2%, 5%, and 8%, respectively. Furthermore, SMA has the ability to reduce the secondary compressive strength compared to other samples, indicating the quality of this material in controlling stress after cracking. Finally, it was indicated that the combined use of these two materials increases the strength parameters.

Keywords: concrete; shape memory alloy fibers; silica fume; mechanical properties; secondary compressive strength

Citation: Xie, Y.; Far, H.; Mortazavi, M.; El-Sherbeeny, A.M. Improving the Mechanical Properties of Concrete Mixtures by Shape Memory Alloy Fibers and Silica Fume. *Buildings* **2024**, *14*, 1709. https://doi.org/10.3390/buildings14061709

Academic Editor: Tomasz Sadowski

Received: 24 March 2024
Revised: 20 May 2024
Accepted: 3 June 2024
Published: 7 June 2024

1. Introduction

As a fundamental component of sustainable development, concrete's improved performance and durability under diverse conditions are essential for advancing construction practices [1–3]. Concrete is a fundamental material in construction, serving as the backbone for erecting skyscrapers, paving roads, building bridges, and tunnel reinforcement, highlighting its vital role in infrastructure [4–6]. Obtaining sustainable development necessitates the optimal utilization of resources and the enhancement of building security and resilience [7,8]. This enhancement can lead to better performance and increased durability of concrete when subjected to a variety of load conditions, including seismic disturbances [9–11]. Therefore, it is crucial to furnish policymakers with enhanced understanding to guide their decision making towards sustainable development and associated infrastructures [12–14]. Concrete's role in sustainable development is deeply intertwined with the use of cement, which forms the foundation of the infrastructure that concrete strengthens and supports.

Cement is the cornerstone of modern construction, being the most extensively utilized material in the industry [15]. Its application in concrete underpins the infrastructure that shapes our cities and lives. Yet, this widespread use comes at a steep ecological price

[16,17]. Greenhouse gas emissions and pollutants play a significant role in environmental degradation [18], and the process of cement production amplifies these issues, such as releasing CO_2 gas into the air [19,20]. About seven percent of the global CO_2 emissions are caused by the industry of Portland cement [21]. People are using more and more cement every day, and the release of CO_2 causes irreparable damage to the environment. It is possible to reduce part of the environmental pollution by replacing pozzolanic materials such as silica fume (SF) instead of ordinary Portland cement (OPC) [22–24]. SF is made of silica that has no definite shape or structure, which comes from the industry that makes ferrosilicon [25]. This material is a gray-white powder that is formed when industrial silicon and ferrosilicon alloys are melted [26,27]. Using SF that is recovered is very important for both the environment and the economy [28]. Also, SF is a key ingredient in high-strength and repaired concretes and is used for dams and other engineering works [29–31]. Pandey and Kumar [32] in a study on SF replaced cement at 2.5, 5, 7.5, and 10 percent and examined the strength parameters in short- and long-term periods. Results showed that the application of 7.5 percent SF recorded the best performance, and curing has a significant effect on increasing the strength parameters. Luo et al. [33] have used SF as an additive in concrete at 2.5, 5, 7.5, and 10 percent. It was revealed that the use of 10% SF caused the greatest increase in splitting tensile and compressive strength, and this material significantly affects the properties of concrete. Wan et al. [34] have also used SF as an additive in concrete; SF has replaced cement in percentages of 3, 6, and 9, and according to compressive strength tests, they have come to the conclusion that using 9 percent of SF gives more suitable results.

Fibers in concrete serve to enhance its mechanical properties, control cracking, and improve durability. They are essential for creating more resilient and robust structures [35–37]. Shape memory alloy (SMA) is a type of metal alloy that has different mechanical features that are not found in steel used for construction. SMA can be made by various metal combinations; nevertheless, the most common SMA for structural uses is the one made of nickel and titanium metals, as it has higher strength, great corrosion resistance, excellent fatigue characteristics, and a larger strain that can be recovered [38]. SMA shows two different crystal phases: Martensite and austenite. Phase change can happen because of internal stresses or temperature changes [39–41]. Studies have been conducted to explore the application of nickel–titanium (NiTi)-SMA fibers to enhance the mechanical behavior of regular concrete structures [42,43]. Moreover, SMA is common in smart constructions because they can go back to their original shapes after the deformation [44,45]. NiTi-SMA is the most common kind of SMA material with two main mechanical features, superelasticity and shape memory effect (SME), which happen because of the changeable phase changes between two solid phases known as austenite and martensite [46]. Superelasticity is about stress changes that can bring the alloy back to its original shape from ultra-large non-linear elastic deformations when unloaded. Also, SME is a unique property of SMA, which refers to the return of this material to its original shape after applying heat. This phenomenon occurs due to a reversible phase transformation in the material's crystal structure, where heating above a certain transition temperature induces a change from a deformed martensitic phase to an austenitic phase, thus recovering the original shape [47–49]. Li et al. [50] examined the recovery force of concrete mixtures with SMA, which indicated that SMA fiber reduced the recovery speed from deflecting and that hotter temperatures removed the remaining composite changes. The optimal strain range for civil structures was proposed as 1–3% by Choi et al. [51], who examined the temperature hysteresis features of SMA composites, such as residual stresses and recovery. Additionally, the relationship between energy change and crack closure was explored by Sherif et al. [52] and Otsuka and Ren [53] in SMA-reinforced mixtures, suggesting a way to track crack expansion. According to the studies of Choi et al. [54,55], the ability to repair cracks was comparable for straight and dog-bone SMA fiber, which also enhanced the flexural resistance, and the residual stress of SMA fiber had a significant impact on the crack-repairing ability. Wang et al. [55] have used SMA fibers in percentages of 0.5, 0.75, and 1 in

concrete mixtures and showed that with increasing the content of fibers in concrete, the number of slumps decreases, and SMA increases the compressive, splitting tensile, flexural strength, and modulus of elasticity. Furthermore, these fibers showed good resistance to cracking in concrete. Dehghani and Aslani [56] examined the effects of incorporating pseudoelastic SMA fibers into concrete, focusing on the material's flexural and compressive characteristics. The study compared the properties of pseudoelastic SMA-reinforced concrete and SMA-reinforced concrete using different volumes of fibers. Using 2D digital image correlation, the study methodically assessed crack patterns and widths. It was found that pseudoelastic SMA-reinforced concrete, while less strong in flexure, displayed superior toughness and deflection capabilities compared to SMA-reinforced concrete. Also, compressive strength and elasticity were slightly lower in concrete mixtures containing pseudoelastic SMA, but the stress-strain behavior remained comparable to those just modified by SMA. A very effective way to enhance the mechanical properties of materials and increase the remaining life of loaded components is to use composite materials or additives in different ways [57,58]. The application of SF and SMA can be a highly effective strategy to augment the mechanical properties of concrete and, thereby, extend the service life of structural components.

Research Objectives

Due to the extensive advantages of using SMA in concrete structures and the limited research conducted on it, examining the application of SMA fibers in concrete structures is one of the primary and fundamental purposes of the current research. On the other hand, a significant aspect of this research is the concurrent utilization of SMA and SF in concrete structures, which has not been explored before. Therefore, this research is unique and special in this regard. It should also be noted that by using SF in concrete structures, other objectives of this research are reducing cement consumption and using mineral and waste materials in concrete, aiming to reduce environmental pollution resulting from cement production. In addition, performing the secondary compressive strength test of samples containing these two additives separately and hybridly is another important goal of this research. This test aimed to identify the reasons for failure and examine the reliability of the initial test outcomes. To investigate these aspects, this laboratory-based study involves the use of SMA and SF at different percentages, both individually and simultaneously, in concrete structures. Various mechanical tests, including compressive strength, splitting tensile strength, and flexural strength, were performed over a 28-day period to assess the results.

2. Materials and Methods

2.1. Materials

The Portland cement used is type 2 and conforms to the ASTM C150/C150M-21 standard [59], and Table 1 exhibits its chemical analysis. The water used in this study was potable and free of any harmful substances based on ASTM C94/C94M-15 standard [60]. The specific weight of coarse aggregate is 2410 kg/m^3, and the specific weight of fine aggregate is 2680 kg/m^3, and the grading chart of these two materials is presented in Figure 1. Also, the aggregates used are according to the ASTM C637-20 standard [61]. Sampling in this research was conducted according to the BS1881 standard [62]. After complete mixing, the concrete was poured into the molds, and after 24 h of storage in the laboratory environment, in accordance with the BS1881 standard, it was removed from the molds and transferred to the storage tank at a temperature of 23 °C. The chemical analysis of used SF and SMA is shown in Table 1, and a view of them is represented in Figure 2. Moreover, Table 2 indicates the characteristics of the SMA used in this research.

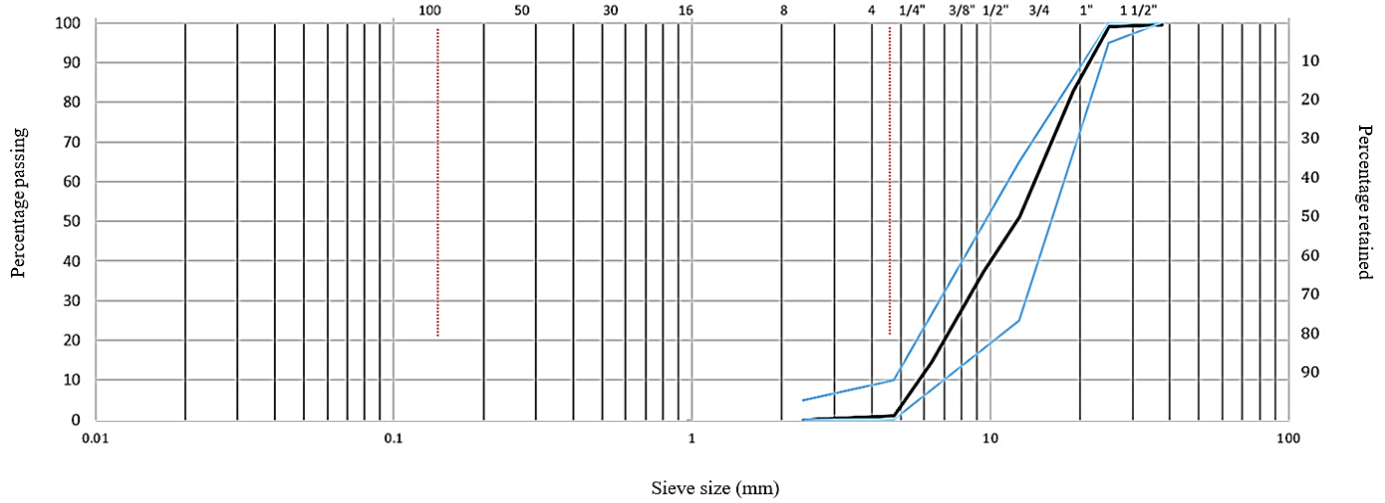

(**a**)

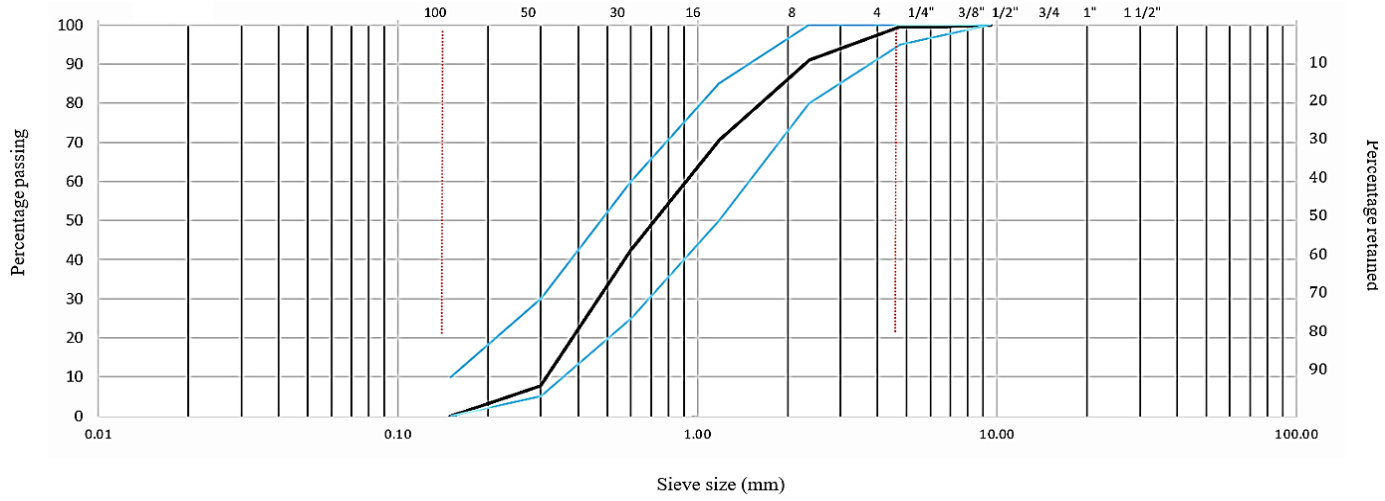

(**b**)

Figure 1. Distribution chart of particle sizes for: (**a**) sand; (**b**) gravel. Note: Blue lines: gradation limits, black line: particle gradation

Table 1. Chemical characteristics of SF, SMA, and cement.

Compounds	SF	SMA	Cement
SiO_2	94.38	-	-
Fe_2O_3	1.22	-	4.19
Al_2O_3	2.75	-	4.95
CaO	-	-	62.28
SO_3	-	-	2.2
MgO	0.54	-	3.2
Na_2O	-	-	0.6
K_2O	-	-	0.45
P_2O_5	-	-	1.18
Ti	-	44.25	-
Ni	-	55.71	-
C	-	0.004	-
O	-	0.04	-
L.O.I	1.11	0.0001	0.0001

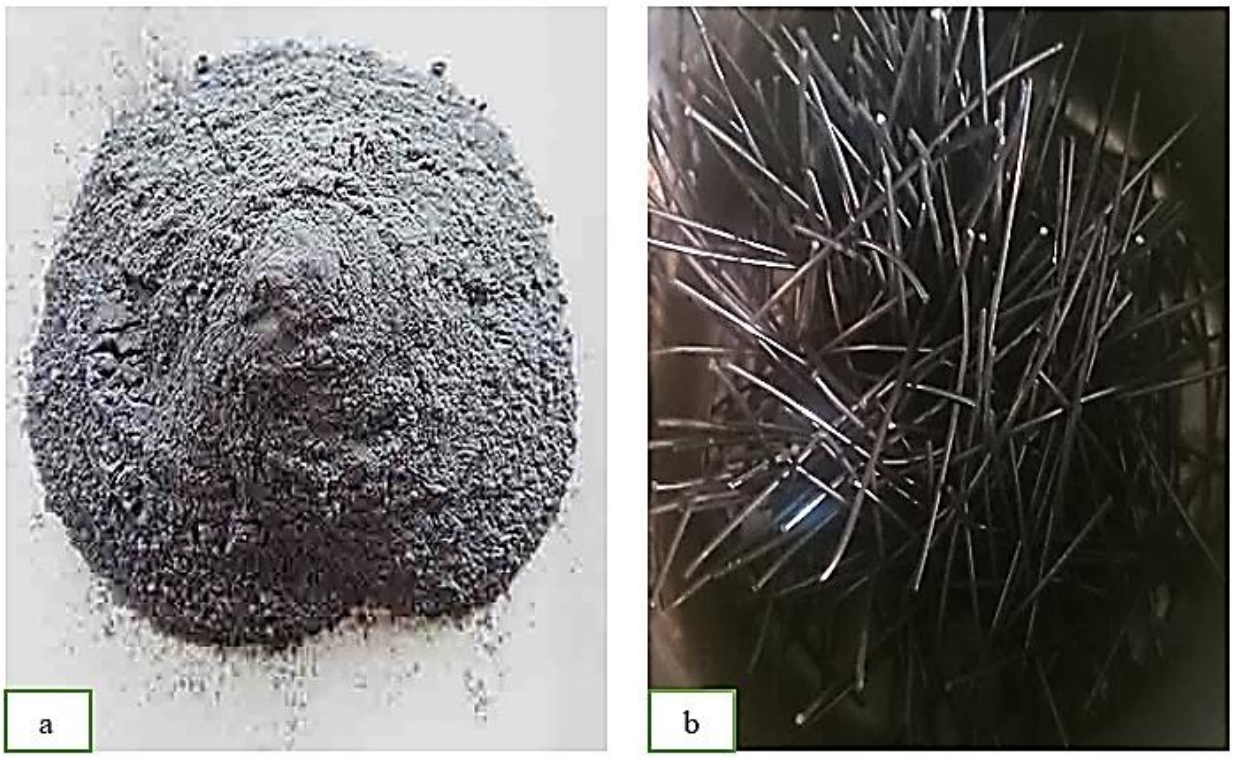

Figure 2. A view of used additives: (**a**) SF; (**b**) SMA.

Table 2. Characteristics of applied SMA.

Characteristics	Unit	Results
Wire diameter	mm	1
Wire length	mm	50
Young's modulus martensite	GPa	28–40
Young's modulus austenite	GPa	70–98
Yield strength martensite	MPa	70–140
Yield strength austenite	MPa	195–690
Ability to change the length	%	10.15
Shape	-	Straight
Color	-	Dark

2.2. Experimental Procedure

2.2.1. Mixture Proportioning

In Table 3, the mix design for producing 1 cubic meter of concrete is presented. In all the mix designs, the water-to-cement (W/C) ratio was 0.4, and the grade of cement was 400 kg/m^3. In this research, 8 mix designs were studied, in which SMA with a specific weight of 6450 kg/m^3 was used separately in volume percentages of 0.1, 0.2, and 0.3 in three mix designs. SF with a specific weight of 2250 kg/m^3 was used in 5, 7.5, and 10 percentages and by weight as a substitute for cement. In one mix design, SF and SMA fiber were used in combination, and another mix design was the control mixture (OPC). In addition, to improve mechanical properties and slump control, superplasticizers were used in all the mix designs.

Table 3. Various mix designs for constructing 1 m^3 of concrete mixtures.

Mix ID	Cement (kg)	Sand (kg)	Gravel (kg)	SF (kg)	SMA (kg)	W/C
OPC	400	1100	740	-	-	0.4
SF5	380	1100	740	20	-	0.4
SF7.5	370	1100	740	30	-	0.4
SF10	360	1100	740	40	-	0.4
SMA0.1	400	1100	740	-	6.5	0.4
SMA0.2	400	1100	740	-	13	0.4
SMA0.3	400	1100	740	-	19.5	0.4
SF10SMA0.3	360	1100	740	40	19.5	0.4

2.2.2. Testing of Specimens

After preparing and mixing the concrete in the mixer according to ASTM C192/C192M-14 standard [63], ASTM C143 standard [64] were applied to perform the slump test, and then the concrete was transferred into the molds. After 24 h, the samples were taken out of the mentioned molds and transferred to the holding pond until 28 days later. They were then tested for compressive strength according to the BS EN 12390-3 standard [65], splitting tensile strength based on the ASTM C496-96 standard [66] and flexural strength test based on the ASTM C293/C293M-16 standard [67]. It is also worth mentioning that the secondary compressive strength test was conducted for samples without SMA immediately after the compressive strength test on broken samples. However, all samples containing SMA were first heated for 24 h to a temperature of 60 °C in the oven according to ISO 834-14 [68] for preheating, and then they were again placed under the concrete breaker jack to perform the compressive strength test for the second time. The technical process was exactly the same as the compressive strength test that was performed on the samples first. The purpose of performing this hot reloading on samples containing SMA was to stimulate the temperature control property of this material and to find the effect of applying heat to the resulting samples. The choice of this temperature was made considering the phase change temperature of SMA derived from its chemical analysis and also considering the fact that the said temperature causes less damage to the cement bond matrix and the inner layers of concrete [69].

The UPV test was also performed based on the ASTM C215-14 standard [70]. To calculate the modulus of elasticity (MOE), the wave speed was first calculated from Equation (1). In this equation, V is the longitudinal pulse velocity, L is the path length (sample length), and t is the pulse transmission time. Then, MOE was calculated from Equation (2), where E_d is dynamic MOE, ρ is the density of the concrete sample, and μ is concrete Poisson's ratio, which is considered 0.2 in this test [71].

$$V = L/t, \tag{1}$$

$$E_d = \rho V^2 \frac{(1+\mu)(1-2\mu)}{(1+\mu)}, \tag{2}$$

In Figure 3, the ultrasonic pulse velocity measurement device can be seen. It should be noted that in order to reduce laboratory errors and increase the accuracy of the results, 5 samples were produced from each mix design for each test.

Figure 3. A view of the ultrasonic concrete tester.

3. Results and Discussion

3.1. Slump and Density Test Results

In this research, varying quantities of the superplasticizer were utilized to standardize the slump values across all mix designs. This approach was adopted to minimize the influence of slump variations on the strength parameters. According to Figure 4, which shows slump test outcomes, it can be seen that all the mix designs of this research were in a specific and limited range. The changes in the density of the mix designs of this research are reported in Figure 5, based on which it can be said that the use of SF and SMA does not have much effect on the density of the samples, which is because the density of cement and SF are close to each other and low percentages of SMA were used in the concrete mix. In the research of Aslani et al. [41], where SMA was used in the concrete mixture, it was reported that the use of SMA did not have much effect on the slump of the samples.

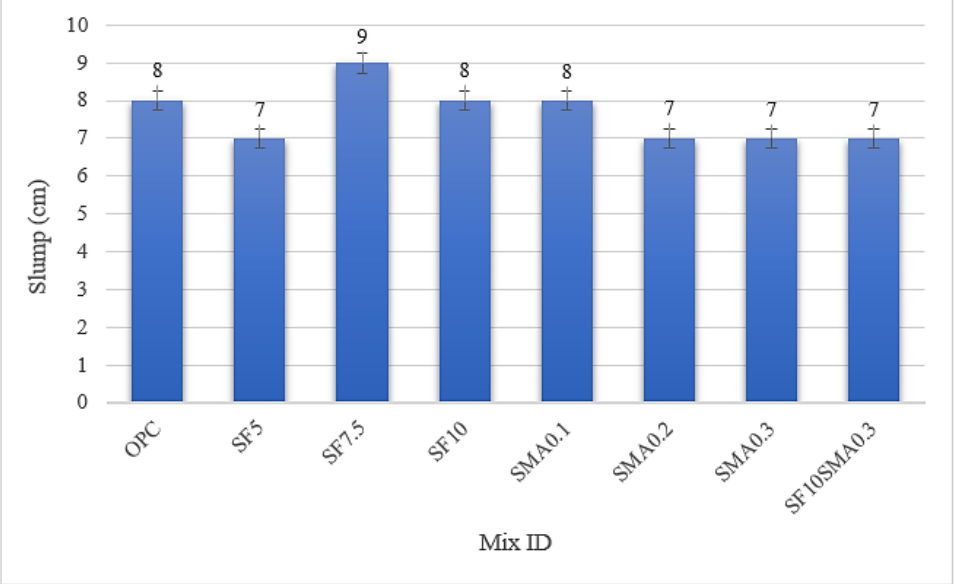

Figure 4. Results of the slump test.

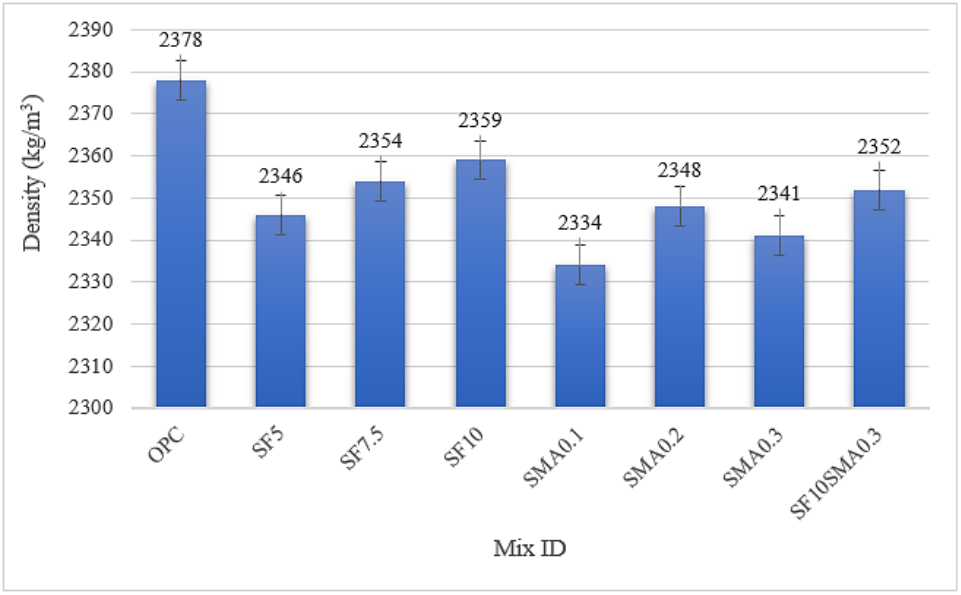

Figure 5. Results of the density test.

3.2. Primary and Secondary Compressive Strength Test Results

In the current research, primary and secondary compressive strength tests were performed for all mix designs in a 28-day period, and Figure 6 displays the results. The results showed using SF can result in an increment in the compressive strength of concrete, and the highest increase is nearly 14% compared to OPC and occurs when 10% of this material is used in the concrete structure. Adding SF to concrete significantly increases the overall surface area in the concrete matrix, leading to enhanced internal surface forces that, in turn, boost the concrete's cohesiveness [72]. Furthermore, by enhancing the properties of the cement paste, SF improves the bond between the aggregates and the cement paste, resulting in a more homogeneous mixture and a reduction in the porosity of concrete [73]. It is obvious that SF reduces the pores of concrete due to the very small particles in its structure and, as a result, reduces the porosity and density of concrete [74]. In addition, the active content of SiO2 in SF is much higher than that of cement, and this causes more C-S-H gel to be produced, which increases the compressive strength [75,76]. SF enhances the strength of OPC-based concrete through a secondary hydration process known as the pozzolanic reaction. This reaction produces additional C-S-H gel, densifies the microstructure, reduces pore sizes, and decreases the content of weaker calcium hydroxide, leading to a more durable and high-performance concrete. Chand et al. [77] reported that by using 15% SF, the compressive strength increased by nearly 15%. Luo et al. [33] have also used SF as an additive in concrete, and the compressive strength results showed that SF can increase the compressive strength by 18%. The use of SMA also increased the compressive strength of concrete in such a way that the use of 0.3% of SMA caused an increase in the compressive strength of nearly 2% compared to the control sample. When Wang et al. [42] also used 0.5% of SMA, the compressive strength increased by nearly 6%. The enhancement in compressive strength is attributed to the elevated content of fibers, in such a way that using more of this material reduces the space around the fibers in concrete's inner layers and increases its resistance to the created loading, so elevated fiber content reduces the stress within the fiber-matrix interface, slowing crack growth and consequently boosting compressive strength [41]. For SF10SMA0.3, compressive strength has increased by more than 11%, and this shows the concurrent application of SF and SMA has a good effect on the compressive strength. In the secondary compressive strength test, it was also determined that, due to the special properties of SMA, the drop in compressive strength in designs containing this material is much less than in other designs. For example, for SF7.5, the secondary compressive strength has been reduced by 32% in comparison with

the primary strength, but for SMA0.2, this value has been recorded at 21%. The reason for this is the ability of SMA to control the residual stress, Also, this material fills the cracks created in the sample by changing its shape, and this has increased the secondary compressive strength. In general, using these fibers with regard to secondary compressive strength in the current research shows SMA fibers have the ability to be used in retrofitting structures and have many uses. This issue has been mentioned in various sources [78,79]. Figure 7a shows the failure of one of the SMA0.3 samples, and the high strength of the sample is evident from its failure angle. This image clearly shows that the bond between cement and other components of concrete is so strong that the aggregates fail when the specimen breaks under load. In concrete mixtures that have a weak cement matrix bond, the aggregates do not yield because they have already failed by yielding the cement areas of the sample. A view of the appearance of the sample containing SMA0.3 under reloading (secondary compressive strength test) can be seen in Figure 7b. Apart from the rupture of the inner layers, this image well depicts the cracks on the outer surface of the sample after reloading. It is worth considering to maintain the apparent integration of the mentioned sample after re-applying the tension on its surface. This is due to the presence of more fibers in the inner layers of the sample, which shows that it is the reason for the cohesion of the concrete body. The little difference in the compressive strength of samples containing fibers with their secondary compressive strength showed that reinforced samples are able to recover part of their lost capacity by applying heat due to the presence of SMA and SME properties of this material. An event that does not occur in concrete containing steel fibers. Steel fibers that fail after bearing the force no longer have the bearing capacity, but SMA bends after loading (due to its higher flexibility than steel fibers) and is able to return to its original state by applying heat. resist the force of the jack and delay the time of failure despite the concrete cracks around it.

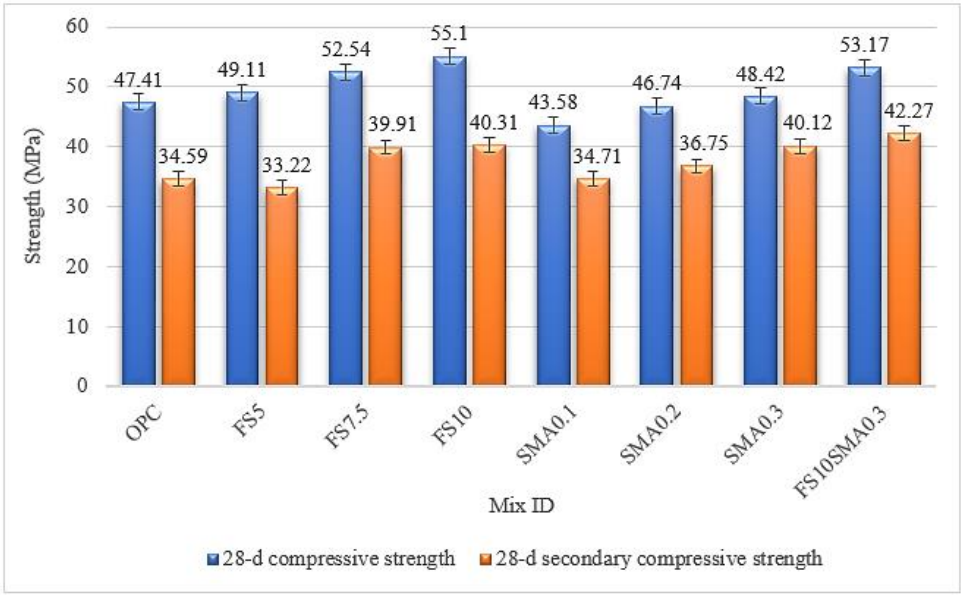

Figure 6. Analysis of primary and secondary compressive strengths.

Figure 7. (**a**) Compressive failure mode; (**b**) secondary compressive failure mode.

3.3. Splitting Tensile and Flexural Strength Test Results

A view of splitting tensile and flexural strength failures is shown in Figure 8, and Figures 9 and 10 indicate the outcomes of these two tests. The results show that the substitution of SF instead of cement significantly affects splitting tensile strength and flexural strength in a way that SF10 has improved these strengths by 7% and 10% in comparison with the OPC, respectively.

SF is a highly active pozzolan because of its very fine particle sizes and very large amount of amorphous silica. SF affects concrete in three main ways: (i) By improving the bonding between aggregates and cement paste, (ii) by reacting with free lime, and (iii) by reducing the pore size and increasing the density of the matrix [73]. The transition zone's properties between aggregates and cement paste particles affect the bonding between cement and aggregate. The thickness of the transition phase in the mortar and the alignment of the CH crystals in it are influenced by adding SF. The transition phase becomes thinner and less oriented with SF than with only OPC. This improves the interfacial or bond strengths, which leads to better durability and mechanical performance [73]. The splitting tensile strength was greatly enhanced by substituting the cement paste with SF in this test, even though W/C was unchanged. A potential explanation was that the cubic compressive strength was boosted by adding SF, which also increased the splitting tensile strength. Alternatively, the cement paste became softer and more tensile by adding SF, which lowered its stiffness compared to the aggregate particle [80].

In a study, Pandey and Kumar [32] used SF in percentages of 2.5, 5, 7.5, and 10 and performed flexural and splitting tensile strength tests on the samples. The results showed that this material increases the flexural strength, and the greatest increase was nearly 12%, and the splitting tensile strength also increased by nearly 8% in the best case. Luo et al. [33] also showed increasing splitting tensile strengths by replacing SF in such a way that the use of 10% of this material caused an increment in splitting tensile strength of about 20%.

SMA can also increase concrete's splitting tensile strength and flexural strength, like many other types of fibers. In this study, the highest rate of growth of these two characteristics happened in SMA0.3, where splitting tensile strength had an increment of more than 5% and flexural strength had an increment of about 8% compared to OPC. A topic that Aslani et al. [41] also confirmed in their research. It should also be mentioned that SF10SMA0.3 acted as the most successful design in the field of flexural strength and was

able to improve this parameter by 12.5% compared to OPC. The splitting tensile strength of this design has also increased by about 7% compared to OPC. It seems that the simultaneous use of SF and SMA is effective and has enhanced the mechanical characteristics of concrete mixtures. The simultaneous use of SF and SMA has resulted in better performance in flexural strength compared to the SF10 and SMA0.3 scenarios, and to some extent, this holds true for splitting tensile strength as well. This indicates that the incorporation of these two additives into the concrete structure is suitable. Considering the compressive strength test results conducted in this research, it can be concluded that the mechanical characteristics of concrete mixtures improve with the concurrent application of SF and SMA in the concrete structure, which was one of the primary objectives of this study. Moreover, by substituting SF for cement in the concrete structure, a significant reduction in cement consumption occurs. This leads to a substantial decrease in greenhouse gas emissions and, additionally, contributes to energy savings.

It should also be noted that in the investigation of flexural strength, the SF10 and SMA0.3 combination demonstrated a slight positive effect, representing a complex interplay between the materials within the concrete matrix. The marginal difference observed in the flexural strength between SF10 and SF10SMA0.3 indicates that while SMA contributes to the composite's properties, its efficiency in conjunction with SF requires further exploration. This could be attributed to potential interactions between the mechanical and structural properties of the concrete, influenced by the combined effects of SF and SMA. Such interactions may result in either a synergistic or antagonistic relationship, affecting the overall performance of the composite material. It is conceivable that the concrete has reached an optimal level of flexural strength enhancement with the current admixture proportions. For instance, the presence of SMA in the mix might diminish the positive effects of SF10, or vice versa. This phenomenon could be due to differences in the mechanical, thermomechanical, or structural properties of the two materials, which may not act as effectively in combination as anticipated. To maximize the benefits of each material, it may be necessary to refine the mixing process or consider alternative materials that could complement each other more effectively. The nuanced interactions between SF and SMA call for a deeper analysis to optimize the composite's performance. This study opens avenues for future research to enhance the understanding of material synergies and their practical applications in concrete technology.

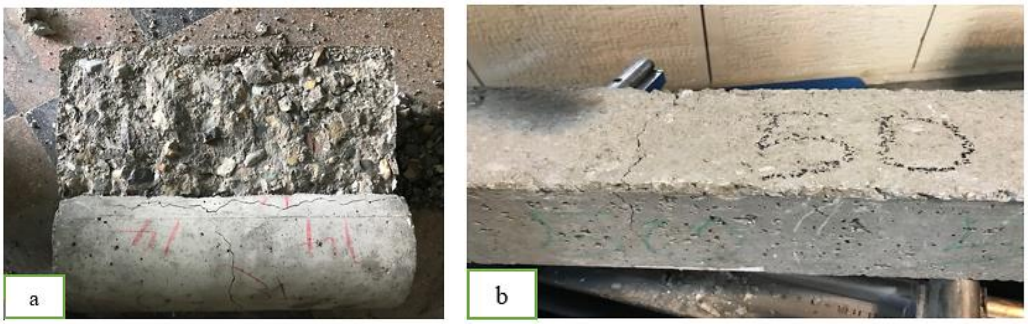

Figure 8. The failure modes for: (**a**) splitting tensile strength and (**b**) flexural strength.

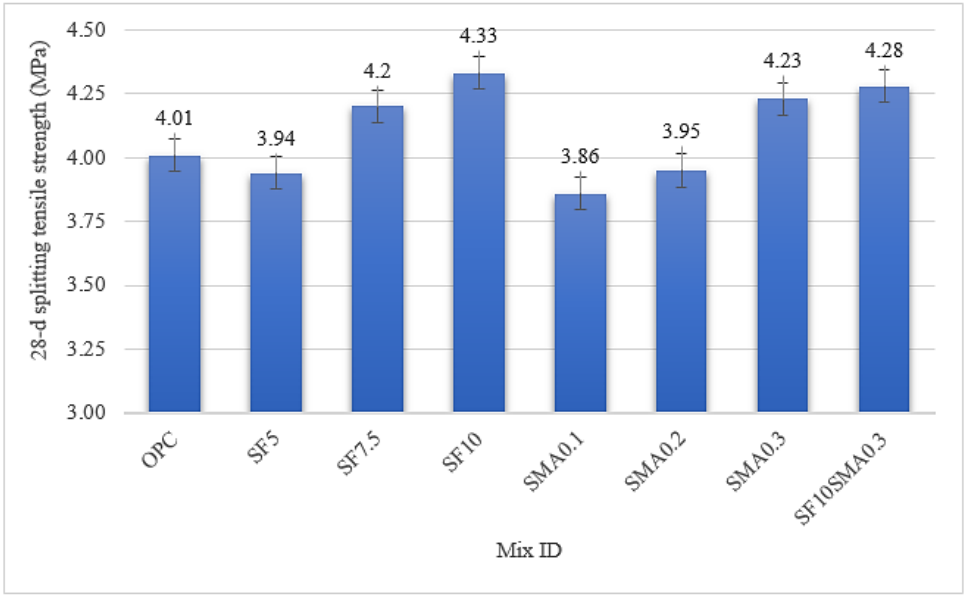

Figure 9. Results of splitting tensile strength.

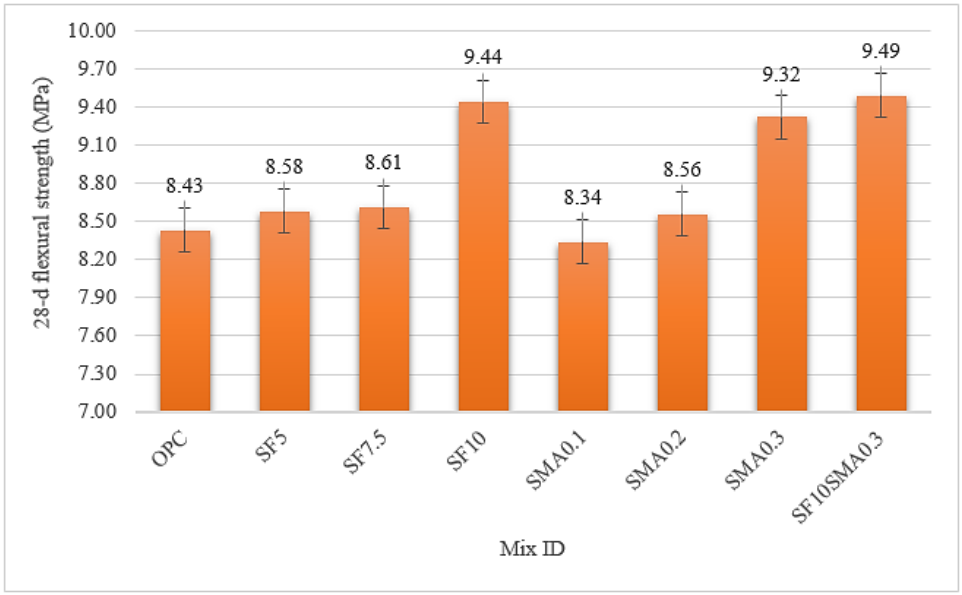

Figure 10. Results of flexural strength test.

3.4. UPV Test Results

In Figure 11, the results of the UPV and MOE of concrete samples are represented side by side in a comparative manner. The MOE of concrete samples has a direct relationship with two parameters: Concrete density and ultrasonic pulse velocity. This test is applied to determine the lifespan of concrete because it indicates the quality of the adhesion of aggregates and cement paste [81,82]. As can be seen from the results, the ultrasonic pulse velocity in the mixture design containing SF is higher than the fiber samples and even the control sample. This observation is indicative of SF's role in enhancing the material's density and microstructure, leading to improved wave transmission. Meanwhile, SF5 and SF7.5 have recorded a lower MOE than the OPC sample, but SF10 has the highest UPV and MOE among all designs, which is expected due to the compressive strength of this design. The use of SF in a paste matrix can lead to improved UPV results by enhancing the material's density and microstructure, resulting in more efficient ultrasonic wave transmission. Furthermore, SF can increase the surface transfer area of fibers within the matrix,

leading to better fiber-matrix interaction and improved mechanical properties of the composite material. Moreover, considering the importance of the interfacial transition zone (ITZ) in influencing UPV values and the mechanical properties of the concrete samples, it should be noted that the ITZ is a critical region that significantly influences the overall performance of reinforced concrete. The improved UPV values in SF-enhanced samples could be partially explained by a denser and more homogenous ITZ, which results from the pozzolanic reaction of SF leading to a refined pore structure and reduced microcracking, resulting in a more efficient transmission of ultrasonic waves. This densification of the ITZ likely contributes to the superior performance of SF samples compared to those blended with SMA.

On the other hand, it can be seen that in samples containing SMA fibers, UPV and MOE decrease as the use of fibers increases. It is expected that the reason for this is the non-ribbed SMA fibers used in this research, which can cause more holes in the concrete sample at connection points than the samples without fibers. The presence of SMA fibers may introduce discontinuities at ITZ, potentially leading to increased porosity and less efficient stress transfer. This could explain the lower UPV and MOE observed in SMA-SF blended samples as opposed to pure SF samples. This test confirms that the addition of SF to SMA has improved the quality of SF10SMA0.3 compared to other designs containing SMA. In addition, considering that the wave speed of all the samples is more than 4000 m/s, the quality of the samples made is evaluated as appropriate according to the standard [83].

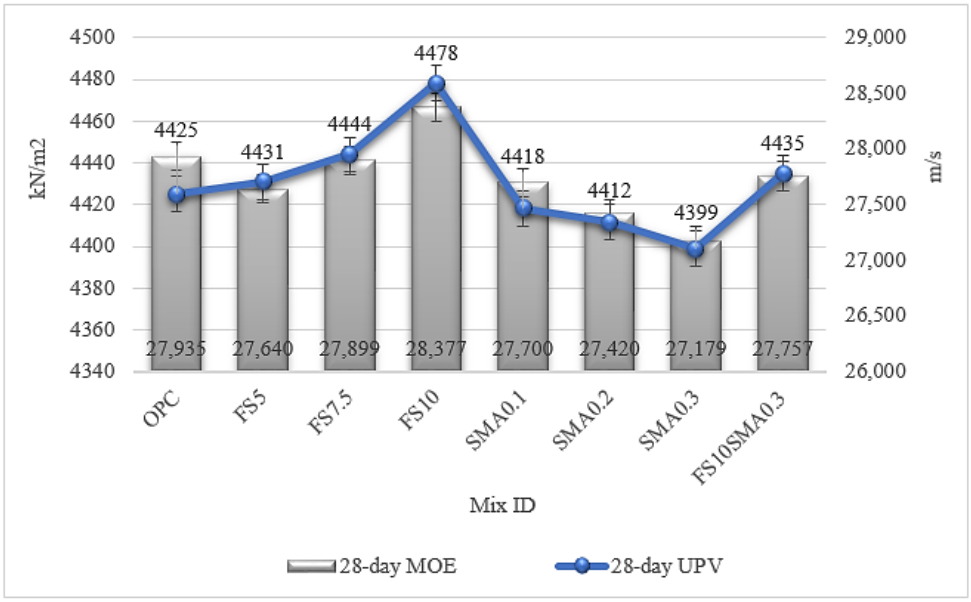

Figure 11. Comparison of UPV and MOE results.

3.5. Correlation Results

Figure 12 also shows the correlation between the compressive strength test outcomes of samples comprising SMA and OPC and the rest of the tests. Based on these graphs and the obtained R^2 value, it was found that the compressive strength of samples comprising SMA is closely related to the secondary compressive, splitting tensile, and flexural strengths of mixtures containing these fibers, but compressive strength is less related to density. As indicated in Figure 12, the correlation coefficients between compressive strength and secondary compressive, flexural, and splitting tensile strengths of concrete samples containing SMA are 0.8419, 0.7663, and 0.7879. Considering the slope of these correlation plots, it becomes evident that SMA has the capability to consistently enhance the mechanical characteristics of concrete mixtures. So that this issue corresponds with the results of the tests. Figure 13 also shows the correlation of the compressive strength of mixtures containing SF and OPC with secondary compressive strength, density, splitting

tensile strength, and flexural strength. Considering the obtained R-squared amounts as represented in Figure 13, which are 0.8135 for secondary compressive, 0.4923 for flexural strength, and 0.7333 for splitting tensile for concrete samples containing SF, it is evident that there is a significant correlation between the compressive strength of concrete with secondary compressive and splitting tensile strength when replacing SF instead of cement, but this correlation is less between compressive strength results and their flexural strength, and density.

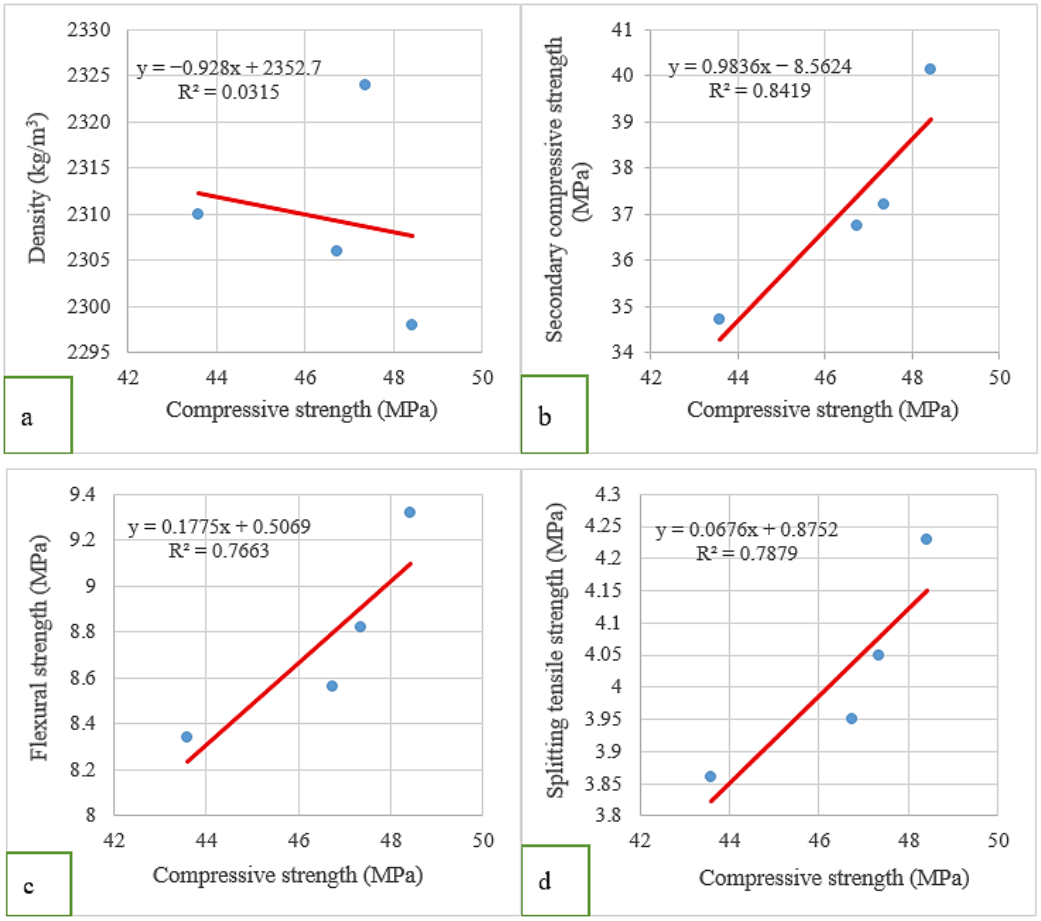

Figure 12. Correlation between compressive strength of OPC and samples comprising SMA for: (**a**) density, (**b**) secondary compressive strength, (**c**) flexural strength, and (**d**) splitting tensile strength.

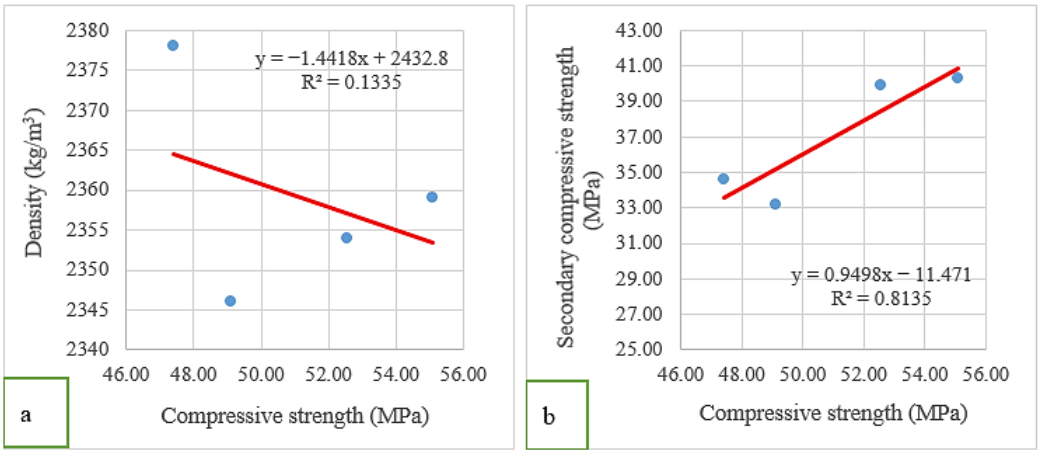

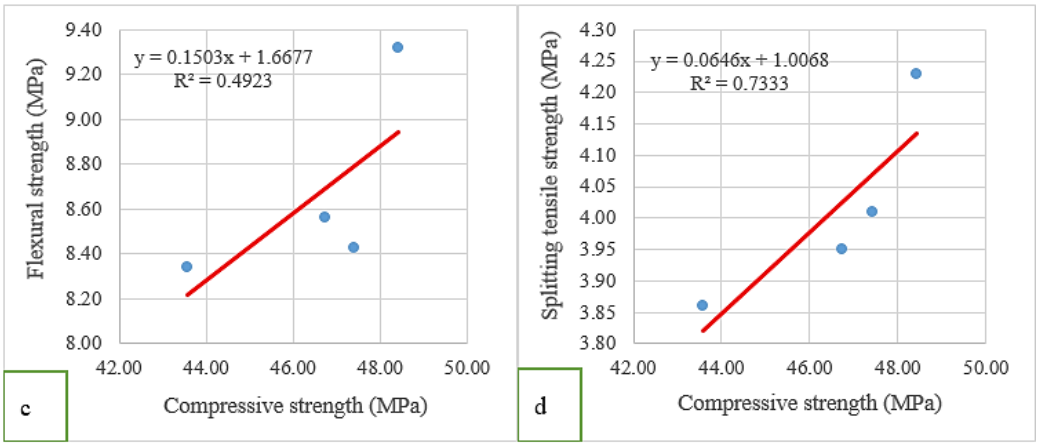

Figure 13. Correlation between compressive strength of OPC and samples comprising SF for: (**a**) density, (**b**) secondary compressive strength, (**c**) flexural strength, and (**d**) splitting tensile strength.

4. Conclusions

In order to increase the quality and efficiency of concrete mixtures, various types of pozzolans and fibers can be used in the concrete structure. In this research, an attempt was made to improve the mechanical properties of concrete by using industrial SF pozzolan and SMA fiber. These two additives were studied together and separately in 8 mix designs, and compressive strength, splitting tensile strength and flexural strength tests, secondary compressive strength, and UPV tests were performed on them over a period of 28 days. The most important results of this study are:

- Replacing SF with cement in the concrete structure by strengthening the cement paste makes the bonding between the aggregates stronger and improves the strength parameters. The highest of this improvement is related to SF10, which caused a 14% increment in compressive strength, 7% in splitting tensile strength, and 10% in flexural strength of the samples compared to OPC.
- The higher content of SMA indicates the most significant improvements in the mechanical properties of concrete mixtures, so that SMA0.3 has improved compressive strength by 2%, splitting tensile strength by 5.5%, and flexural strength by 8% in comparison with OPC.
- Another ability that SMA creates in concrete is due to the properties of reversibility and superelasticity of this material, which show well in the secondary compressive strength test. The decreased rate of secondary compressive strength compared to the primary in mixtures containing SMA after heating is much lower than in other samples. For example, in SMA0.3, the secondary compressive strength has decreased by only 16%, but in OPC, this value is equal to 28%.
- SF10SMA0.3 positively affects improving the mechanical characteristics of concrete mixtures. So that the compressive strength has an increment of 11%, the splitting tensile strength by 6.7%, and the flexural strength by 12.5% in comparison with OPC, it can be said that the concurrent application of these two modifiers in concrete structures has been successful.
- UPV in the mix design containing SF is higher than the fiber samples and even the control sample, so that SF10, just like the compressive strength test, has registered the highest UPV and MOE among all designs.
- The obtained R2 value indicates that the compressive strength of samples comprising SMA has a very high correlation with the secondary compressive, splitting tensile, and flexural strengths of mixtures containing these fibers. In addition, the compressive strength of the mix designs comprising SF has an acceptable correlation with the secondary compressive and splitting tensile strengths.

- For future research directions, the long-term influence of SMA and SF on concrete is recommended to be investigated. A wider array of mix designs incorporating both SF and SMA can also be explored to fully assess their synergistic effects on the mechanical properties of concrete. Moreover, various machine learning methods [84–86] can be developed to predict the behavior of SMA and SF-reinforced concrete.

Author Contributions: Conceptualization, Y.X. and H.F.; methodology, M.M. and A.M.E.-S.; formal analysis, M.M.; investigation, Y.X. and M.M.; resources, A.M.E.-S.; data curation, M.M.; writing—original draft preparation, M.M.; writing—review and editing, A.M.E.-S.; visualization, Y.X.; supervision, Y.X. and H.F.; project administration, H.F. All authors have read and agreed to the published version of the manuscript.

Funding: This work was Supported by the Opening Project of Sichuan Province University Key Laboratory of Bridge Non-destruction Detecting and Engineering Computing. The authors extend their appreciation to King Saud University, Saudi Arabia, for funding this work through Researchers Supporting Project number (RSP2024R133), King Saud University, Riyadh, Saudi Arabia.

Data Availability Statement: The datasets generated during and/or analyzed during the current study are available from the corresponding author upon reasonable request.

Conflicts of Interest: Author Yuanyong Xie was employed by the company Municipal Design Research Institute of Chongqing Design Group Co., Ltd. The remaining authors declare that the research was conducted in the absence of any commercial or financial relationships that could be construed as a potential conflict of interest.

References

1. Han, S.; Zheng, D.; Mehdizadeh, B.; Nasr, E.A.; Khandaker, M.U.; Salman, M.; Mehrabi, P. Sustainable design of self-consolidating green concrete with partial replacements for cement through neural-network and fuzzy technique. *Sustainability* **2023**, *15*, 4752.
2. Liu, J.; Mohammadi, M.; Zhan, Y.; Zheng, P.; Rashidi, M.; Mehrabi, P. Utilizing artificial intelligence to predict the superplasticizer demand of self-consolidating concrete incorporating pumice, slag, and fly ash powders. *Materials* **2021**, *14*, 6792.
3. Tapas, M.; Song, Z.; Mortazavi, M.; Moghaddam, F.; Sirivivatnanon, V. Particle Packing Theory in Ultra-sustainable Concrete with High SCM Content. 2021. Available online: https://opus.lib.uts.edu.au/bitstream/10453/162391/2/Particle%20Packing%20Theory%20in%20Ultra-sustainable%20Concrete%20with%20High%20SCM.pdf (accessed on).
4. Shabbir, F.; Bahrami, A.; Ahmad, I.; Shakouri Mahmoudabadi, N.; Iqbal, M.; Ahmad, A.; Özkılıç, Y.O. Experimental and Numerical Investigation of Construction Defects in Reinforced Concrete Corbels. *Buildings* **2023**, *13*, 2247.
5. Liu, B.; Yang, H.; Karekal, S. Effect of water content on argillization of mudstone during the tunnelling process. *Rock Mech. Rock Eng.* **2020**, *53*, 799–813.
6. Yang, H.; Song, K.; Zhou, J. Automated recognition model of geomechanical information based on operational data of tunneling boring machines. *Rock Mech. Rock Eng.* **2022**, *55*, 1499–1516.
7. Razi, S.; Wang, X.; Mehreganian, N.; Tootkaboni, M.; Louhghalam, A. Application of mean-force potential lattice element method to modeling complex structures. *Int. J. Mech. Sci.* **2023**, *260*, 108653. https://doi.org/10.1016/j.ijmecsci.2023.108653.
8. Samadi, M.; Jahan, N. Determining the effective level of outrigger in preventing collapse of tall buildings by IDA with an alternative damage measure. *Eng. Struct.* **2019**, *191*, 104–116.
9. Vahid, R.; Farnood Ahmadi, F.; Mohammadi, N. Earthquake damage modeling using cellular automata and fuzzy rule-based models. *Arab. J. Geosci.* **2021**, *14*, 1274.
10. Samadi, M.; Jahan, N. Comparative study on the effect of outrigger on seismic response of tall buildings with braced and RC wall core. I: Optimum level and examining modal response spectrum analysis reliability. *Struct. Des. Tall Spec. Build.* **2021**, *30*, e1848.
11. Souri, O.; Mofid, M. Seismic evaluation of concentrically braced steel frames equipped with yielding elements and BRBs. *Results Eng.* **2023**, *17*, 100853.
12. Asgari, M.; Khodakarami, M.; Vahdani, R. The effect of topographic irregularities on seismic response of the concrete rectangular liquid storage tanks incorporating soil–structure–liquid interaction. *Iran. J. Sci. Technol. Trans. Civ. Eng.* **2020**, *44*, 1179–1197.
13. Jaradat, Y.; Far, H.; Mortazavi, M. A Mathematical Approach for Predicting Sufficient Separation Gap between Adjacent Buildings to Avoid Earthquake-Induced Pounding. *Civ. Eng. J.* **2023**, *9*, 2370–2398.
14. Hu, D.; Sun, H.; Mehrabi, P.; Ali, Y.A.; Al-Razgan, M. Application of artificial intelligence technique in optimization and prediction of the stability of the walls against wind loads in building design. *Mech. Adv. Mater. Struct.* **2023**, 1–18.

15. He, H.; Qiao, H.; Sun, T.; Yang, H.; He, C. Research progress in mechanisms, influence factors and improvement routes of chloride binding for cement composites. *J. Build. Eng.* **2024**, *86*, 108978. https://doi.org/10.1016/j.jobe.2024.108978.
16. Adiguzel, D.; Tuylu, S.; Eker, H. Utilization of tailings in concrete products: A review. *Constr. Build. Mater.* **2022**, *360*, 129574. https://doi.org/10.1016/j.conbuildmat.2022.129574.
17. Demir Şahin, D.; Eker, H. Effects of Ultrafine Fly Ash against Sulphate Reaction in Concrete Structures. *Materials* **2024**, *17*, 1442.
18. Esmaili, A.; Oshanreh, M.M.; Naderian, S.; MacKenzie, D.; Chen, C. Assessing the spatial distributions of public electric vehicle charging stations with emphasis on equity considerations in King County, Washington. *Sustain. Cities Soc.* **2024**, *107*, 105409. https://doi.org/10.1016/j.scs.2024.105409.
19. Sousa, V.; Bogas, J.A.; Real, S.; Meireles, I. Industrial production of recycled cement: Energy consumption and carbon dioxide emission estimation. *Environ. Sci. Pollut. Res.* **2023**, *30*, 8778–8789.
20. Liu, Y.; Wang, B.; Fan, Y.; Yu, J.; Shi, T.; Zhou, Y.; Song, Y.; Xu, G.; Xiong, C.; Zhou, X. Effects of reactive MgO on durability and microstructure of cement-based materials: Considering carbonation and pH value. *Constr. Build. Mater.* **2024**, *426*, 136216. https://doi.org/10.1016/j.conbuildmat.2024.136216.
21. El-Feky, M.; Kohail, M.; El-Tair, A.M.; Serag, M. Effect of microwave curing as compared with conventional regimes on the performance of alkali activated slag pastes. *Constr. Build. Mater.* **2020**, *233*, 117268.
22. Hamed, Y.R.; Elshikh, M.M.Y.; Elshami, A.A.; Matthana, M.H.; Youssf, O. Mechanical properties of fly ash and silica fume based geopolymer concrete made with magnetized water activator. *Constr. Build. Mater.* **2024**, *411*, 134376.
23. Singh, S.; Ransinchung, G.; Kumar, P. Effect of mineral admixtures on fresh, mechanical and durability properties of RAP inclusive concrete. *Constr. Build. Mater.* **2017**, *156*, 19–27.
24. Paul, D.K.; Gnanendran, C.T. Characterization of lightly stabilized granular base materials using monotonic and cyclic load flexural testing. *J. Mater. Civ. Eng.* **2016**, *28*, 04015074.
25. Mozafarjazi, M.; Rabiee, R. Experimental and numerical study on the load-bearing capacity, ductility and energy absorption of RC shear walls with opening containing zeolite and silica fume. *Eng. Solid Mech.* **2024**, *12*, 237–246.
26. Villar-Cociña, E.; Rodier, L.; Savastano, H.; Lefrán, M.; Rojas, M.F. A comparative study on the pozzolanic activity between bamboo leaves ash and silica fume: Kinetic parameters. *Waste Biomass Valorization* **2020**, *11*, 1627–1634.
27. Sharaky, I.; Megahed, F.; Seleem, M.; Badawy, A. The influence of silica fume, nano silica and mixing method on the strength and durability of concrete. *SN Appl. Sci.* **2019**, *1*, 575.
28. Ghasemi, A.; Naser, M.Z. Tailoring 3D printed concrete through explainable artificial intelligence. *Structures* **2023**, *56*, 104850. https://doi.org/10.1016/j.istruc.2023.07.040.
29. Choudhary, R.; Gupta, R.; Alomayri, T.; Jain, A.; Nagar, R. Permeation, corrosion, and drying shrinkage assessment of self-compacting high strength concrete comprising waste marble slurry and fly ash, with silica fume. *Structures*, **2021**, *33*, 971–985.
30. Eker, H.; Bascetin, A. Influence of silica fume on mechanical property of cemented paste backfill. *Constr. Build. Mater.* **2022**, *317*, 126089.
31. Bakhshi, A.; Sedghi, R.; Hojati, M. A Preliminary Study on the Mix Design of 3D-Printable Engineered Cementitious Composite. In Proceedings of the Tran-SET 2021, Online, 3–4 June 2021; pp. 199–211. https://doi.org/10.1061/9780784483787.021
32. Pandey, A.; Kumar, B. Effects of rice straw ash and micro silica on mechanical properties of pavement quality concrete. *J. Build. Eng.* **2019**, *26*, 100889.
33. Luo, T.; Hua, C.; Liu, F.; Sun, Q.; Yi, Y.; Pan, X. Effect of adding solid waste silica fume as a cement paste replacement on the properties of fresh and hardened concrete. *Case Stud. Constr. Mater.* **2022**, *16*, e01048.
34. Wan, Z.; He, T.; Chang, N.; Yang, R.; Qiu, H. Effect of silica fume on shrinkage of cement-based materials mixed with alkali accelerator and alkali-free accelerator. *J. Mater. Res. Technol.* **2023**, *22*, 825–837.
35. Cui, D.; Wang, L.; Zhang, C.; Xue, H.; Gao, D.; Chen, F. Dynamic Splitting Performance and Energy Dissipation of Fiber-Reinforced Concrete under Impact Loading. *Materials* **2024**, *17*, 421.
36. Shakouri Mahmoudabadi, N.; Bahrami, A.; Saghir, S.; Ahmad, A.; Iqbal, M.; Elchalakani, M.; Özkılıç, Y.O. Effects of eccentric loading on performance of concrete columns reinforced with glass fiber-reinforced polymer bars. *Sci. Rep.* **2024**, *14*, 1890, doi:10.1038/s41598-023-47609-4.
37. Zhou, Y.; Jiang, Z.; Zhu, X. Predictive Analysis of Concrete Slump Using a Stochastic Search-Consolidated Neural Network. *Heliyon* **2024**, *10*, e30677.
38. Shi, M.; Xu, G.; Zhao, J.; Xu, L. The study on bond-slip constitutive model of shape memory alloy fiber-reinforced concrete. *Constr. Build. Mater.* **2024**, *418*, 135395.
39. Abou-Elfath, H. Ductility characteristics of concrete frames reinforced with superelastic shape memory alloys. *Alex. Eng. J.* **2018**, *57*, 4121–4132.
40. Cladera, A.; Weber, B.; Leinenbach, C.; Czaderski, C.; Shahverdi, M.; Motavalli, M. Iron-based shape memory alloys for civil engineering structures: An overview. *Constr. Build. Mater.* **2014**, *63*, 281–293.
41. Aslani, F.; Liu, Y.; Wang, Y. Flexural and toughness properties of NiTi shape memory alloy, polypropylene and steel fibres in self-compacting concrete. *J. Intell. Mater. Syst. Struct.* **2020**, *31*, 3–16.
42. Wang, Y.; Aslani, F.; Valizadeh, A. An investigation into the mechanical behaviour of fibre-reinforced geopolymer concrete incorporating NiTi shape memory alloy, steel and polypropylene fibres. *Constr. Build. Mater.* **2020**, *259*, 119765.
43. Aslani, F.; Liu, Y.; Wang, Y. The effect of NiTi shape memory alloy, polypropylene and steel fibres on the fresh and mechanical properties of self-compacting concrete. *Constr. Build. Mater.* **2019**, *215*, 644–659.

44. Li, H.; Liu, Z.-Q.; Ou, J.-P. Experimental study of a simple reinforced concrete beam temporarily strengthened by SMA wires followed by permanent strengthening with CFRP plates. *Eng. Struct.* **2008**, *30*, 716–723.
45. Li, L.; Li, Q.; Zhang, F. Behavior of smart concrete beams with embedded shape memory alloy bundles. *J. Intell. Mater. Syst. Struct.* **2007**, *18*, 1003–1014.
46. Gur, S.; Frantziskonis, G.N.; Muralidharan, K. Atomistic simulation of shape memory effect (SME) and superelasticity (SE) in nano-porous NiTi shape memory alloy (SMA). *Comput. Mater. Sci.* **2018**, *152*, 28–37.
47. Li, H.; Liu, Z.-Q.; Ou, J.-P. Behavior of a simple concrete beam driven by shape memory alloy wires. *Smart Mater. Struct.* **2006**, *15*, 1039.
48. Deng, Z.; Li, Q.; Sun, H. Behavior of concrete beam with embedded shape memory alloy wires. *Eng. Struct.* **2006**, *28*, 1691–1697.
49. Fang, C.; Wang, W.; He, C.; Chen, Y. Self-centring behaviour of steel and steel-concrete composite connections equipped with NiTi SMA bolts. *Eng. Struct.* **2017**, *150*, 390–408.
50. Li, H.; Liu, Z.-Q.; Ou, J.-P. Study on reinforced concrete beams strengthened using shape memory alloy wires in combination with carbon-fiber-reinforced polymer plates. *Smart Mater. Struct.* **2007**, *16*, 2550.
51. Choi, E.; Cho, S.-C.; Hu, J.W.; Park, T.; Chung, Y.-S. Recovery and residual stress of SMA wires and applications for concrete structures. *Smart Mater. Struct.* **2010**, *19*, 094013.
52. Sherif, M.M.; Tanks, J.; Ozbulut, O.E. Acoustic emission analysis of cyclically loaded superelastic shape memory alloy fiber reinforced mortar beams. *Cem. Concr. Res.* **2017**, *95*, 178–187.
53. Otsuka, K.; Ren, X. Physical metallurgy of Ti–Ni-based shape memory alloys. *Prog. Mater. Sci.* **2005**, *50*, 511–678. https://doi.org/10.1016/j.pmatsci.2004.10.001.
54. Choi, E.; Joo Kim, D.; Youn, H.; Nam, T.-h. Repairing cracks developed in mortar beams reinforced by cold-drawn NiTi or NiTiNb SMA fibers. *Smart Mater. Struct.* **2015**, *24*, 125010. https://doi.org/10.1088/0964-1726/24/12/125010.
55. Choi, E.; Kim, D.; Lee, J.-H.; Ryu, G.-S. Monotonic and hysteretic pullout behavior of superelastic SMA fibers with different anchorages. *Compos. Part B Eng.* **2017**, *108*, 232–242. https://doi.org/10.1016/j.compositesb.2016.09.080.
56. Dehghani, A.; Aslani, F. Flexural toughness and compressive stress–strain behaviour of pseudoelastic shape memory alloy fibre reinforced concrete. *Constr. Build. Mater.* **2022**, *332*, 127372. https://doi.org/10.1016/j.conbuildmat.2022.127372.
57. Behseresht, S.; Mehdizadeh, M. Mode I&II SIFs for semi-elliptical crack in a cylinder wrapped with a composite layer. In Proceedings of the 28th Annual International Conference of Iranian Society of Mechanical Engineers-ISME2020, Tehran, Iran, 27–29 May 2020; pp. 27–29.
58. Golewski, G.L.; Sadowski, T. Experimental investigation and numerical modeling fracture processes under Mode II in concrete composites containing fly-ash additive at early age. *Solid State Phenom.* **2012**, *188*, 158–163.
59. *ASTM C150/C150M-21*; Standard Specification for Portland Cement. ASTM International: West Conshohocken, PA, USA, 2021.
60. *ASTM C94/C94M-15*; Standard Specification for Ready-Mixed Concrete. ASTM International: West Conshohocken, PA, USA, 2015.
61. *ASTM C637-20*; Standard Specification for Aggregates for Radiation-Shielding Concrete. ASTM International: West Conshohocken, PA, USA, 2020.
62. *BS1881*; Method for determination of compressive strength of concrete cubes. BSI: London, UK, 1983.
63. *ASTM C192/C192M-14*; Standard Practice for Making and Curing Concrete Test Specimens in the Laboratory. ASTM International: West Conshohocken, PA, USA, 2015.
64. *ASTM C143-78*; Standard Test Method for Slump of Portland Cement Concrete. ASTM International: West Conshohocken, PA, USA, 2017.
65. *BS EN 12390-3*; Testing Hardened Concrete Compressive Strength of Test Specimens. BSI: London, UK, 2019.
66. *ASTM C496-96*; Standard Test Method for Splitting Tensile Strength of Cylindrical Concrete Specimens. ASTM International: West Conshohocken, PA, USA, 2017.
67. *ASTM C293/C293M-16*; Standard Test Method for Flexural Strength of Concrete (Using Simple Beam With Center-Point Loading). ASTM International: West Conshohocken, PA, USA, 2016.
68. *ISO 834-14*; Fire-resistance tests—Elements of building construction. ISO: Geneva, Switzerland, 2019.
69. Nematzadeh, M.; Tayebi, M.; Samadvand, H. Prediction of ultrasonic pulse velocity in steel fiber-reinforced concrete containing nylon granule and natural zeolite after exposure to elevated temperatures. *Constr. Build. Mater.* **2021**, *273*, 121958.
70. *ASTM C215-14*; Standard Test Method for Fundamental Transverse, Longitudinal, and Torsional Resonant Frequencies of Concrete Specimens. ASTM International: West Conshohocken, PA, USA, 2020.
71. Neville, A.M.; Brooks, J.J. *Concrete Technology*; Longman Scientific & Technical England: London, UK, 1987; Volume 438.
72. Malviya, B.; Sealey, B. Use of Microsilica in High Performance Precast Concrete. In *The Masterbuilder*; Hachette Book Group: New York, NY, USA, 2016.
73. Siddique, R. Utilization of silica fume in concrete: Review of hardened properties. *Resour. Conserv. Recycl.* **2011**, *55*, 923–932.
74. Behnood, A.; Ziari, H. Effects of silica fume addition and water to cement ratio on the properties of high-strength concrete after exposure to high temperatures. *Cem. Concr. Compos.* **2008**, *30*, 106–112.
75. Smarzewski, P. Influence of silica fume on mechanical and fracture properties of high performance concrete. *Procedia Struct. Integr.* **2019**, *17*, 5–12.
76. Mardani-Aghabaglou, A.; Sezer, G.İ.; Ramyar, K. Comparison of fly ash, silica fume and metakaolin from mechanical properties and durability performance of mortar mixtures view point. *Constr. Build. Mater.* **2014**, *70*, 17–25.

77. Chand, G.; Happy, S.K.; Ram, S. Assessment of the properties of sustainable concrete produced from quaternary blend of portland cement, glass powder, metakaolin and silica fume. *Clean. Eng. Technol.* **2021**, *4*, 100179.
78. Jung, C.-Y.; Lee, J.-H. Crack closure and flexural tensile capacity with SMA fibers randomly embedded on tensile side of mortar beams. *Nanotechnol. Rev.* **2020**, *9*, 354–366.
79. Lee, J.-H.; Lee, K.-J.; Choi, E. Flexural capacity and crack-closing performance of NiTi and NiTiNb shape-memory alloy fibers randomly distributed in mortar beams. *Compos. Part B Eng.* **2018**, *153*, 264–276.
80. Li, L.G.; Kwan, A.K. Adding limestone fines as cementitious paste replacement to improve tensile strength, stiffness and durability of concrete. *Cem. Concr. Compos.* **2015**, *60*, 17–24.
81. Bellum, R.R.; Muniraj, K.; Madduru, S.R.C. Investigation on modulus of elasticity of fly ash-ground granulated blast furnace slag blended geopolymer concrete. *Mater. Today Proc.* **2020**, *27*, 718–723.
82. Jena, T.; Panda, K. Mechanical and durability properties of marine concrete using fly ash and silpozz. *Adv. Concr. Constr.* **2018**, *6*, 47.
83. *Indian Standard, Non-Destructive Testing of Concrete, Part 1: Ultrasonic Pulse Velocity*; Bureau of Indian Standard: New Delhi, India, 1992.
84. Do, Q.; Le, T.; Le, C. Uncovering Critical Causes of Highway Work Zone Accidents Using Unsupervised Machine Learning and Social Network Analysis. *J. Constr. Eng. Manag.* **2024**, *150*, 04023168.
85. Talebi Khameneh, R.; Elyasi, M.; Özener, O.Ö.; Ekici, A. A non-clustered approach to platelet collection routing problem. *Comput. Oper. Res.* **2023**, *160*, 106366. https://doi.org/10.1016/j.cor.2023.106366.
86. Qiu, Y.; Wang, J. A Machine Learning Approach to Credit Card Customer Segmentation for Economic Stability. In Proceedings of the 4th International Conference on Economic Management and Big Data Applications, ICEMBDA 2023, Tianjin, China, 27–29 October 2023.